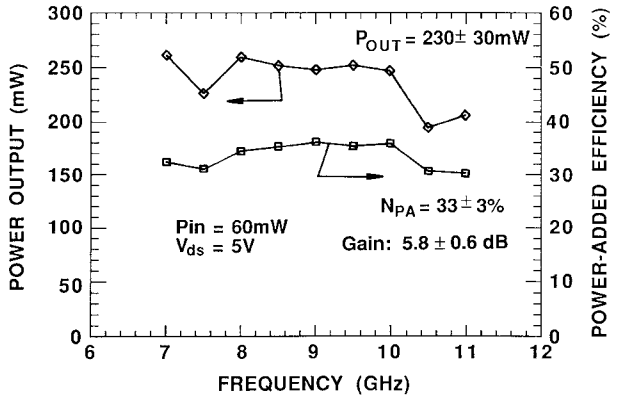

Fig. 3. Power performance of wide-band GaInAs MISFET amplifier stage Tuned for highest efficiency over 7–11 GHz band.

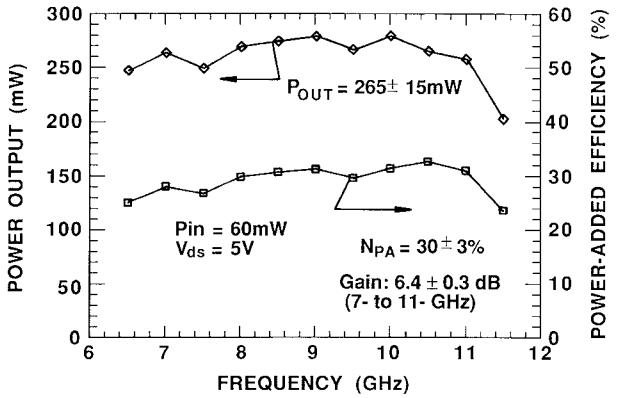

Fig. 4. Power performance of wide-band GaInAs MISFET amplifier stage. Tuned for highest power output over 7–11 GHz band.

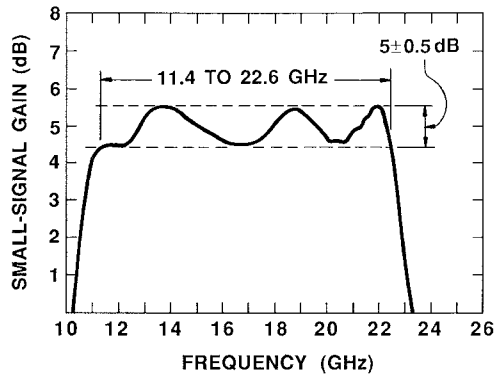

Fig. 5. Wide-band performance of GaInAs MISFET amplifier stage using 0.7-μm-gate-length MISFET.

nal gain of 5 ± 0.5 dB over the bandwidth of 11.4 to 22.6 GHz. Again, no corrections were made for circuit losses.

V. Summary and Conclusions

The combination of high power density, wide bandwidth, and high power-added efficiency obtained demonstrates the potential of GaInAs MISFET's in wide-band amplifier applications. Further development, including submicrometer gate lengths and the use of improved device geometries, will result in significant improvements to the already good performance of GaInAs MISFET wide-band power amplifiers.

Acknowledgment

The authors gratefully acknowledge the contributions of S. D. Colvin, who fabricated the GaInAs MISFET's, and of J. P. Paczkowski and D. R. Capewell, who grew the GaInAs wafers.

References

[1] A. Cappy, B. Carnez, R. Fauquembergues, G. Salmer, and E. Constant, "Comparative potential performance of Si, GaAs, GaInAs, and InAs submicrometer FET's," *IEEE Trans. Electron Devices*, vol ED-27, p. 2158, 1980.

[2] M. A. Littlejohn, J. R Hauser, and T. H Glisson, "Velocity-field characteristics of $Ga_xIn_{1-x}As_yP_{1-y}$ quaternary alloys," *Appl Phys. Lett.*, vol. 30, no. 5, p. 242, 1977.

[3] P D. Greene, S. A. Wheeler, A. R. Adams, A. N El-Sabbhey, and C. N. Ahmed, "Background carrier concentration and electron mobility in LPE-grown $Ga_xIn_{1-x}As_yP_{1-y}$ layers," *Appl Phys. Lett*, vol. 35, p. 78, 1979

[4] R. F. Leheny, A A. Ballman, J. C. DeWinter, R. E. Nahory, and M A. Pollock, "Compositional dependence of the low-field mobility in $Ga_xIn_{1-x}As_yP_{1-y}$," *J. Elec. Mat.*, vol. 9, p. 561, 1980.

[5] S. Y. Narayan, J. P. Paczkowski, S. T. Jolly, E. P. Bertin, and R. Smith, "Growth and characterization of $Ga_xIn_{1-x}As_yP_{1-y}$ and $Ga_{0.47}In_{0.53}As$ for microwave device applications," *RCA Rev.*, vol 42, p. 491, Dec. 1981.

[6] K. Kajiyama, Y. Mizushima, and S. Sakata, "Schottky-barrier heights of n-$Ga_xIn_{1-x}As$ diodes," *Appl. Phys. Lett*, vol. 23, p. 458, 1973

[7] P D. Gardner, S. Y. Narayan, and Y-H. Yun, "Characteristics of the low-temperature-deposited SiO_2-$Ga_{0.47}In_{0.53}As$ metal/insulator/semiconductor interface," *Thin Solid Films*, vol 117, p. 173, 1984.

[8] Umesh Sharma, "Electrical characteristics of photodeposited SiO_2/Si interface," *RCA Rev.*, vol 47, pp 551–577, Dec 1986

[9] P. D. Gardner, S. Y. Narayan, S. D. Colvin, and Y-H. Yun, "$Ga_{0.47}In_{0.53}As$ metal insulator field-effect transistors (MISFETs) for microwave frequency applications," *RCA Rev.*, vol 42, p. 542, Dec 1981

[10] P. D. Gardner *et al.*, "$Ga_{0.47}In_{0.53}As$ deep depletion and inversion mode MISFETs," in *Proc. Inst. Phys. Conf.* (Ser. No. 65), 1983, ch. 5, p 399.

[11] P. D Gardner *et al.*, "Self-aligned-gate GaInAs microwave MISFETs," *IEEE Electron Device Lett.*, vol EDL-7, p. 363, June 1986.

[12] L. C Upadhyayula, P. D Gardner, S. G Liu, and S Y Narayan, "Inversion-mode GaInAs ring oscillators," *IEEE Electron Device Lett.*, vol. EDL-7, p. 390, June 1986.

[13] P. D. Gardner, D Bechtle, S Yegna Narayan, S. D Colvin, and J. Paczkowski, "High-efficiency GaInAs microwave MISFETs," *IEEE Electron Device Lett*, vol EDL-8, pp. 443–446, Sept. 1987.

[14] H. Fukui, "Determination of the basic device parameters of a GaAs MESFET," *Bell Syst. Tech. J*, vol 58, no 3, pp. 771–797, Mar. 1979.

[15] S T. Hsu, "A simple method to determine series resistance and *K*-factor of an MOS field effect transistor," *RCA Rev.*, vol 44, pp. 424, 1983

[16] R. A Pucel, H. A. Haus, and H Statz, "Signal and noise properties of GaAs microwave FETs," *Adv Electron Electron Physics*, vol. 38, pp. 195–265, 1975.

Reactances of Slotline Short and Open Circuits on Alumina Substrate

JERZY CHRAMIEC

***Abstract*—Resonant techniques have been employed in order to determine the equivalent normalized reactance of slotline planar short circuits and open circuits realized on alumina substrates. Data for slotline short circuits are presented in a graph covering a wide range of normalized slot widths. Characteristics of several slotline open circuits are given demonstrating their resonant behavior and the resulting bandwidth limitation. As**

Manuscript received September 28, 1988; revised April 20, 1989.

The author is with the Institute of Telecommunication, Technical University of Gdańsk, Majakowskiego 11/12, 80-952 Gdańsk, Poland.

IEEE Log Number 8929892.

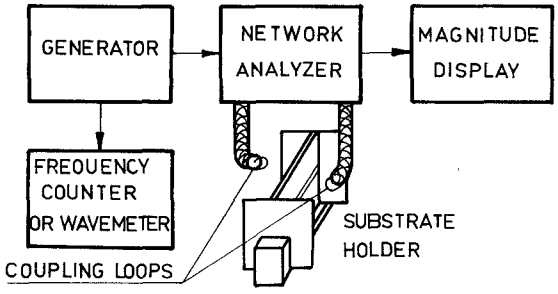

Fig. 1. Experimental setup.

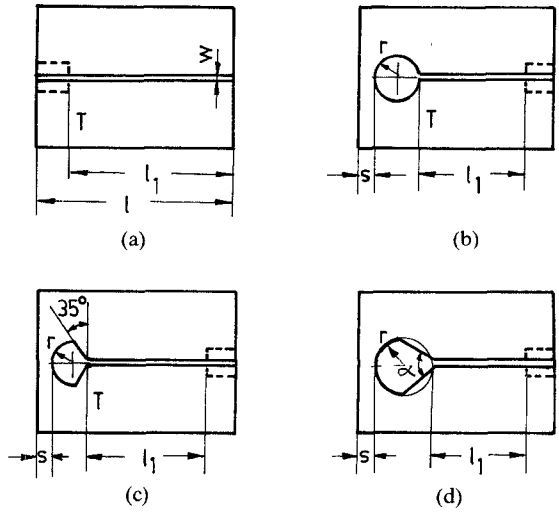

Fig. 2 Slotline test patterns.

an example of an application, the design of broad-band microstrip–slotline transitions employing experimentally characterized slotline open circuits is outlined.

I. Introduction

In the design of slotline circuits, planar short and open circuits are the most frequently encountered discontinuities. Short-end reactance characteristics have been reported [1] for substrate relative permittivities of 12 and 20. Data for slotline open circuits are practically nonexisting.

The purpose of this paper is to report on a resonant technique employed to characterize these discontinuities as well as to present some results useful for the design of slotline circuits on alumina or similar substrates. These include the graph of the planar short-circuit equivalent reactance given for a large range of normalized slot widths and the frequency characteristics of several slotline open circuits. One of the measured open circuits has been employed in the design of broad-band microstrip–slotline transitions.

II. Measurement Setup and Method

Resonant techniques are well established in the characterization of transmission line discontinuities [2], [3]. The experimental setup used in this work is shown in Fig. 1. It makes it possible to determine the resonant frequencies of a given slotline circuit using the transmission method. Weak coupling with the test structure is provided by small coupling loops placed on opposite sides of the substrate. Fig. 2 shows the slotline patterns used. The continuous lines show the initial pattern whereas the broken lines

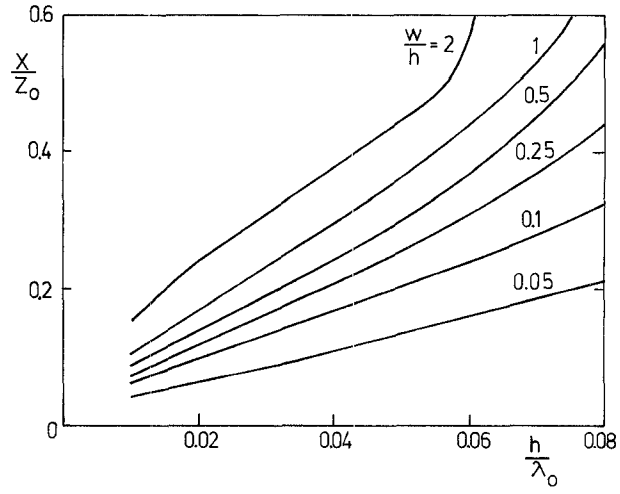

Fig. 3 Measured reactances of slotline short end on alumina substrate.

indicate the modifications obtained by gluing a very thin conductive foil.

The general resonance condition for these circuits is

$$\frac{X_1}{X_0}+\frac{X_2+Z_0\tan\beta l_1}{Z_0-X_2\tan\beta l_1}=0. \tag{1}$$

X_1 and X_2 are the equivalent discontinuity reactances loading the uniform slotline segment l_1; β and Z_0 represent the slotline phase constant and the characteristic impedance, respectively.

Alumina substrates of several dimensions were used in the experiments. Substrate samples exhibiting relative permittivity value were selected using Howell's method [4]. Resonant frequency measurements were performed on nonmodified patterns of Fig. 2(a) with slotline ends short-circuited by perpendicular conductive plates, i.e., $X_1 = X_2 = 0$. The results made it possible to prepare graphs of the correction factor, by which the slotline wavelength computed from [5, formulas 5.32 and 5.33] should be multiplied to increase the accuracy. Then, measurements on slotline circuits including the discontinuity to be characterized were made and the discontinuity normalized reactance was calculated from (1) with the use of corrected resonant wavelengths.

III. Experimental Results

Modified test patterns of Fig. 2(a) served to determine the equivalent reactance of slotline planar short circuits. The results are shown in Fig. 3. Compared with the data for $\epsilon_r = 12$ and $\epsilon_r = 20$ [1], the measured reactance is slightly lower for wide slots and higher for narrow slots.

The equivalent reactance of circular open circuits has been measured on the patterns of Fig. 2(b) and computed with the use of Fig. 3. Sample results are presented in Fig. 4, showing clearly the resonant behavior of these discontinuities. These results indicate that for very broad band applications, the dimensions of circular open circuits should be carefully chosen. The actual bandwidth depends on the required value of X/Z_0, but it cannot exceed 2.5 octaves in the case of presented open circuits.

Fig. 5 shows the characteristics of broad-band nonuniform slotline resonators shaped as in Fig. 2(c). Such structures are recommended in the vicinity of microstrip line (see, for example, Fig. 7(a)) as they disturb to a lesser extent the microstrip ground plane. In one case, Fig. 5 also provides a comparison of the characteristics of two identical resonators placed at different distances from the perpendicular conductive wall and thus exhibiting different end effects. Finally in Fig. 6 are given the

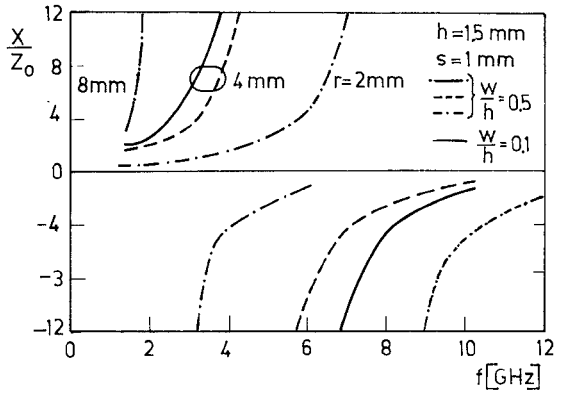

Fig. 4 Measured reactances of slotline circular open circuits on alumina substrate.

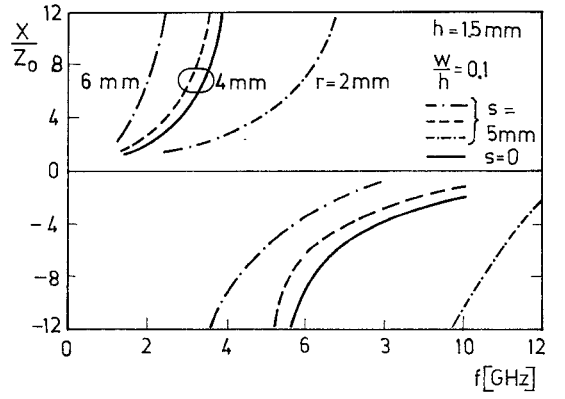

Fig 5. Measured reactances of slotline nonuniform resonators of Fig. 2(c)

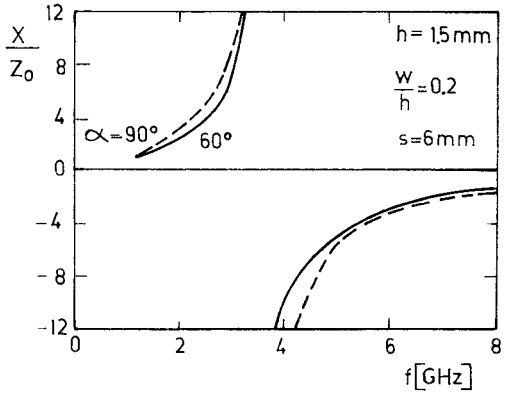

Fig. 6. Measured reactances of slotline nonuniform resonator of Fig. 2(d).

characteristics of two nonuniform resonators dimensioned as in Fig. 2(d) with different values of the angle α.

IV. Example of Application: Design of Broad-Band Microstrip–Slotline Transition

A broad-band microstrip–slotline transition is shown in Fig. 7(a) with the subscript m referring to its microstrip side. The usual equivalent circuit [5] of this transition is given in Fig. 7(b). In the equivalent circuit of Fig. 7(c), all of the components have been transformed to the microstrip side. The input reflection coefficient Γ equals

$$\Gamma = \frac{R_s - Z_{0m} + j(X_m + X_s)}{R_s + Z_{0m} + j(X_m + X_s)} \tag{2}$$

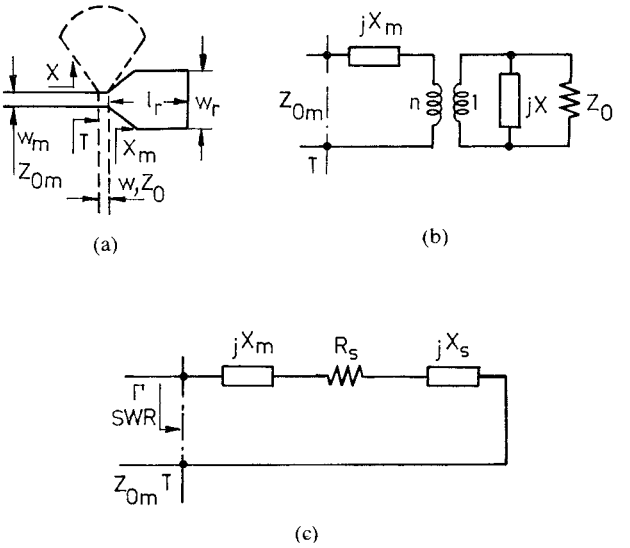

Fig 7. (a) Broad-band microstrip–slotline transition. (b) Equivalent circuit (c) Equivalent circuit after transformation of all components to the microstrip side

where

$$R_s = \frac{n^2 Z_0 X^2}{Z_0^2 + X^2} \qquad X_s = \frac{n^2 Z_0^2 X}{Z_0^2 + X^2}. \tag{3}$$

As n and Z_0 are slowly varying functions of frequency, the transition bandwidth limitation results mostly from the frequency dependence of X and X_m. A through-hole microstrip short circuit may ensure $X_m \simeq 0$; however, the data from the preceding section show that X always exhibits a limited bandwidth. To design a broad-band transition, one may attempt to realize slotline and microstrip resonators providing mutual cancellation of X_m and X_s [6].

An additional constraint stems from the fact that both resonators should not overlap. The experiments and calculations show that in the case of the slotline resonator of Fig. 2(d), this limits the allowable value of α to 60°. It has been verified experimentally that the mutual effect of resonators on their input reactance is negligible far from the resonant frequency, i.e., in the range where the compensation of X_m and X_s should be particularly effective.

To design a 1.5–6 GHz transition, the 60° resonator characterized in Fig. 6 has been employed. The computed characteristics of R_s and X_s are given in Fig. 8, the approximate value of n having been calculated from [5, formulas 6.3–6.7]. The experimental characteristic of a nonuniform microstrip resonator shaped as in Fig. 7(a) is also included. The SWR characteristic of such a transition computed with the use of (2) is represented by the broken-line curve in Fig. 9.

Experimental characteristics have been measured on a test circuit containing two cascade-connected transitions separated by a slotline section 12 mm long, two good-quality microstrip—SMA transitions, and an SMA load of SWR < 1.08. Two-octave bandwidth performance has been obtained, slightly worse than that computed for a single transition. These results compare favorably with the ones given in [7]. This microstrip–slotline transition has been subsequently scaled to a 0.7-mm-thick alumina substrate. The measured SWR of two such cascade-connected transitions is

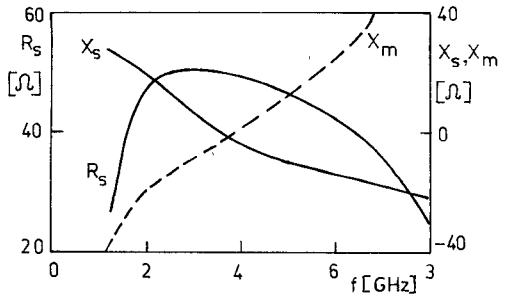

Fig. 8. Frequency characteristics of R_s, X_s, X_m. $l_r = 6.5$ mm, $w_r = 7.5$ mm.

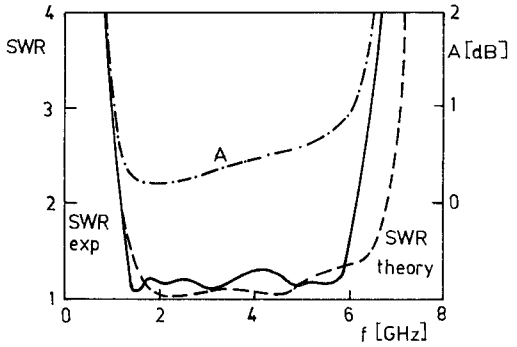

Fig. 9. Theoretical SWR characteristics of single microstrip–slotline transition and experimental characteristics of two cascade-connected transitions. A: insertion loss. $h = 1.5$ mm, $\epsilon_r = 9.8$.

below 1.45 in the frequency range 2 to 12.7 GHz with a local increase to 1.6 in the vicinity of 8 GHz. The achieved bandwidth is comparable to that reported by Schüppert [6] for a similar transition. The midband performance of the realized transitions is, however, somewhat better, which is attributed to the inclusion of the slotline–microstrip voltage transformation ratio n in the modeling.

V. Conclusions

A resonant technique has been described that allows the accurate measurement of slotline short- and open-circuit equivalent reactances. Numerous experimental results have been given for circuits on an alumina substrate ($\epsilon = 9.8$). These include a graph of planar short-end reactance for normalized slot width values of 0.05 to 2 as well as the frequency characteristics of several open circuits. It has been demonstrated that these open circuits behave as nonuniform resonators with the resulting bandwidth limitation. A 1.5–6 GHz low SWR microstrip–slotline transition design has been presented that employs one of the measured open circuits. A 2–12.7 GHz transition has been obtained by scaling the first transition to a thinner substrate.

References

[1] J. B. Knorr and J. Saenz, "End effect in shorted slot," *IEEE Trans. Microwave Theory Tech.*, vol. MTT-21, pp. 579–580, 1973.

[2] B. Easter, J. G. Richings, and I. M. Stephenson, "Resonant techniques for the accurate measurement of microstrip properties and equivalent circuits," in *Proc. 3rd European Microwave Conf.*, 1973, paper B. 7.5.

[3] E. Pic and W. J. R. Hoefer, "Experimental characterization of finline discontinuities using resonant techniques," in *IEEE MTT-S Int. Microwave Symp. Dig.*, 1981, pp. 108–110

[4] J. Q. Howell, "A quick, accurate method to measure the dielectric constant of MIC substrates," *IEEE Trans. Microwave Theory Tech.*, vol. MTT-21, pp. 142–143, 1973.

[5] K. C. Gupta, R. Garg and I. J. Bahl, *Microstrip Lines and Slotlines*. Dedham, MA: Artech House, 1979.

[6] B. Schüppert, "Microstrip–slotline transitions: Modeling and experimental investigation," *IEEE Trans. Microwave Theory Tech.*, vol. 36, pp. 1272–1282, 1988.

[7] A. Podcameni and M. L. Coimbra, "Slotline–microstrip transition on iso/anisotropic substrate: A more accurate design," *Electron. Lett.*, vol. 16, pp. 780–781, 1980.

A Moment Method Solution of a Volume–Surface Integral Equation Using Isoparametric Elements and Point Matching

JIAN-MING JIN, STUDENT MEMBER, IEEE, JOHN L. VOLAKIS, SENIOR MEMBER, IEEE, AND VALDIS V. LIEPA, MEMBER, IEEE

***Abstract*—It is shown that traditional subdomain elements such as rectangles and triangles with a pulse expansion basis could lead to inaccuracies when simulating biological scatterers having high permittivities. In this paper, isoparametric elements are used in a moment method implementation to remove modeling inaccuracies of fields and boundaries associated with traditional elements. Numerical results are also given that show the improvement achieved in the scattering solution for high-contrast circular cylinders.**

I. Introduction

A volume–surface integral equation (VSIE) was recently presented [1], [2] for electromagnetic scattering by inhomogeneous cylinders. A moment method (MM) solution of the VSIE was also considered using rectangular and triangular elements with pulse expansion basis functions and point matching. Such a moment method solution, however, becomes inaccurate in the case of scatterers having high permittivities with transverse electric (TE) incidence or high permeabilities with transverse magnetic (TM) incidence. To overcome this difficulty, in this paper we develop a MM solution by employing isoparametric elements.

Isoparametric elements were first introduced in finite element analysis [3]. The main advantage of using such elements is to allow an accurate modeling of arbitrarily shaped geometries. However, it appears that only recently [4] have they been employed in solutions of volume integral equations for electromagnetics. Below we first discuss the inaccuracy associated with traditional solutions of integral equations for penetrable scatterers having high refractive indices. This is followed by the introduction of isoparametric elements and the presentation of the MM solution of the VSIE using such elements. Results are subsequently presented which show the stability of the solution in the case of cylindrical geometries associated with high refractive indices.

II. Discussion of the Integral Equations

In this section we first examine the VSIE for the computation of the internal fields in a cylinder having nonunity relative permittivity ϵ_r and permeability μ_r. Assuming the cylinder has its

Manuscript received November 28, 1988; revised May 4, 1989. This work was supported in part by the NASA Ames Research Center under Grant NAG-2-541.

The authors are with the Radiation Laboratory, Department of Electrical Engineering and Computer Science, University of Michigan, Ann Arbor, MI 48109.

IEEE Log Number 8929926.